Neuron, Vol. 20, 693–707, April, 1998, Copyright ©1998 by Cell Press

# CRIPT, a Novel Postsynaptic Protein that Binds to the Third PDZ Domain of PSD-95/SAP90

**Martin Niethammer,* Juli G. Valtschanoff,† Tarun M. Kapoor,‡ Daniel W. Allison,§ Richard J. Weinberg,† Ann Marie Craig,§ and Morgan Sheng*‖**

*Department of Neurobiology and Howard Hughes Medical Institute
Massachusetts General Hospital and Harvard Medical School
Boston, Massachusetts 02114
†Department of Cell Biology and Anatomy
University of North Carolina
Chapel Hill, North Carolina 27599
‡Department of Chemistry and Chemical Biology
Harvard University
Cambridge, Massachusetts 02138
§Department of Cell and Structural Biology
University of Illinois
Urbana-Champaign, Illinois 61801

## Summary

**The synaptic protein PSD-95/SAP90 binds to and clusters a variety of membrane proteins via its two N-terminal PDZ domains. We report a novel protein, CRIPT, which is highly conserved from mammals to plants and binds selectively to the third PDZ domain (PDZ3) of PSD-95 via its C terminus. While conforming to the consensus PDZ-binding C-terminal sequence (X-S/T-X-V-COOH), residues at the -1 position and upstream of the last four amino acids of CRIPT determine its specificity for PDZ3. In heterologous cells, CRIPT causes a redistribution of PSD-95 to microtubules. In brain, CRIPT colocalizes with PSD-95 in the postsynaptic density and can be coimmunoprecipitated with PSD-95 and tubulin. These findings suggest that CRIPT may regulate PSD-95 interaction with a tubulin-based cytoskeleton in excitatory synapses.**

## Introduction

The clustering and immobilization of receptors and ion channels at specific subcellular sites is believed to be mediated by intracellular proteins that attach these membrane proteins to the cytoskeleton. Furthermore, receptors and ion channels interact with cytoplasmic proteins involved in the modulation (Holmes et al., 1996; Tsunoda et al., 1997; Yu et al., 1997) or in the downstream signaling mechanisms of the receptor/ion channel (Brenman et al., 1996a; reviewed in Sheng and Kim, 1996; Tsunoda et al., 1997). Our understanding of receptor/ion channel–associated protein complexes has expanded rapidly in recent years, especially at the vertebrate neuromuscular junction (NMJ) and more recently in mammalian central excitatory synapses. In particular, the postsynaptic density (PSD) of excitatory synapses is becoming appreciated as a specialized structure in which an array of synaptic membrane proteins is physically linked and functionally coupled to a specific set of cytoskeletal and/or signaling proteins (reviewed in Ehlers et al., 1996; Sheng and Kim, 1996; Brenman and Bredt, 1997; Kennedy, 1997; Kornau et al., 1997; Sheng and Wyszynski, 1997; Ziff, 1997).

Currently occupying central stage in the PSD is a family of proteins homologous to the *Drosophila* protein Discs large (Dlg; Woods and Bryant, 1991). In mammals, this family consists of the prototypical member PSD-95/SAP90 (Cho et al., 1992; Kistner et al., 1993) plus three additional relatives: SAP97/hDlg (Lue et al., 1994; Müller et al., 1995), chapsyn-110/PSD-93 (Brenman et al., 1996b; Kim et al., 1996), and SAP102 (Müller et al., 1996). Proteins of the PSD-95 family are characterized by three N-terminal PDZ domains, an SH3 domain, and a C-terminal guanylate kinase–like (GK) domain, thus making them members of the membrane-associated guanylate kinase (MAGUK) superfamily (Anderson, 1996; Kornau et al., 1997; Sheng and Kim, 1996). Each of the PDZ, SH3, and GK domains can function as a site for protein–protein interaction.

PDZ domains are modular domains that bind to specific C-terminal peptide sequences and are present in many signaling and cytoskeleton-associated molecules (reviewed in Ponting et al., 1997). The PDZ1 and PDZ2 domains of PSD-95 were first shown to bind specifically to the cytoplasmic C termini of Shaker-type $K^+$ channel subunits and NMDA receptor NR2 subunits (Kim et al., 1995; Kornau et al., 1995; Müller et al., 1996; Niethammer et al., 1996), resulting in the clustering of these membrane proteins (Kim et al., 1995, 1996; Hsueh et al., 1997). The C-terminal tetrapeptide sequences of NR2 and Shaker proteins are, respectively, -ESDV and -ETDV, which agrees almost exactly with the PDZ1/2-binding specificity deduced from random peptide library screening (Songyang et al., 1997). A variety of other ligands of PSD-95 PDZ domains have subsequently been identified, mostly from in vitro experiments (Cohen et al., 1996; Matsumine et al., 1996; Horio et al., 1997; Irie et al., 1997; Thomas et al., 1997; Kim et al., 1998). Based on the sequences of these putative interacting proteins as well as direct mutational analysis (Kim et al., 1995), peptide library screening (Songyang et al., 1997), and X-ray crystallography of the PDZ3 domain complexed with a cognate peptide (Doyle et al., 1996), the consensus C-terminal sequence for binding to the PDZ domains of PSD-95 has come to be represented as -X(T/S)XV (where X represents any amino acid). However, this consensus appears to be an oversimplification. For instance, many C termini that conform to the -X(T/S)XV consensus have poor affinity for PSD-95 PDZ domains. Moreover, although the -X(T/S)XV consensus applies to all three PDZ domains, neither Shaker nor NR2 subunits can bind to PDZ3 of PSD-95 (Kim et al., 1995; Kornau et al., 1995; Niethammer et al., 1996); this implies differential recognition of C-terminal sequences by PDZ1/2 and PDZ3. Understanding the basis of this subtle sequence discrimination by PDZ domains would be aided by knowledge of the specific binding partners for PDZ3. In contrast to

‖To whom correspondence should be addressed.

A

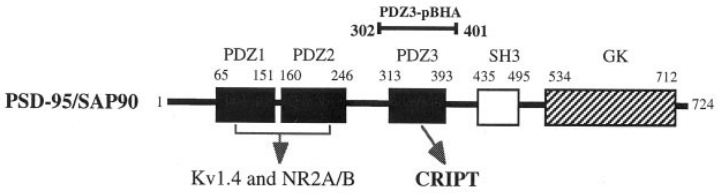


B

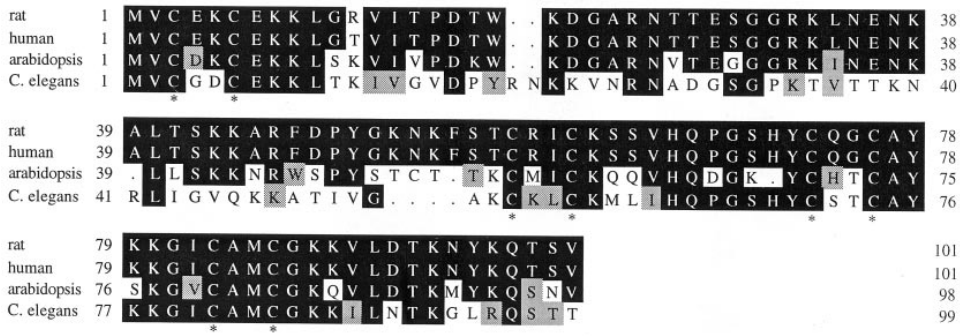


C

| | Rat | Human | Arabid. | C. eleg. |
|---|---|---|---|---|
| Rat | X | 99 (99) | 68 (78) | 48 (65) |
| Human | 99 (99) | X | 68 (78) | 48 (65) |
| Arabid. | 68 (78) | 68 (78) | X | 44 (63) |
| C. eleg. | 48 (65) | 48 (65) | 44 (63) | X |

D

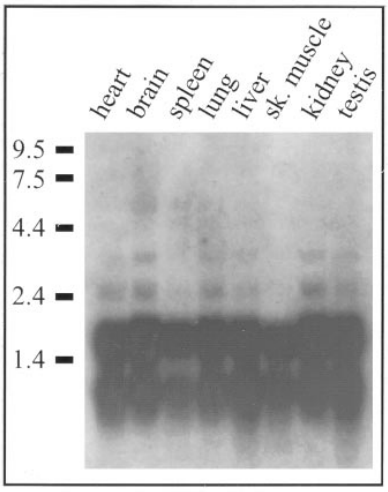


Figure 1. CRIPT Is a Highly Conserved Protein Expressed in Many Tissues

(A) A schematic representation of PSD-95 is shown (small numbers refer to amino acid residues at the boundaries of various domains). CRIPT was isolated from a yeast two-hybrid screen using PDZ3 of PSD-95 as bait (the region contained in the bait is indicated by PDZ3-pBHA).

(B) Alignment of rat CRIPT sequence with proteins encoded by human and *Arabidopsis thaliana* EST sequences and a *C. elegans* genomic sequence. Identical amino acids are boxed in black, conserved changes in gray. The GenBank accession numbers for rat, human, *Arabidopsis, and C. elegans* sequences are AF047384, AA165108, F19988, and Z80215, respectively.

(C) Table showing the percentage identity (similarity) between the sequences shown in (B).

(D) Northern blot of poly(A) mRNA showing CRIPT expression in all tissues examined. The two major bands (~1 and ~2 kb) were overexposed to allow visualization of some minor RNA species.

PDZ1/2, however, little is known about PDZ3-specific ligands with the exception of neuroligin (Irie et al., 1997). Here we report the identification of a novel protein (named CRIPT) that binds selectively to the PDZ3 domain of PSD-95. Binding specificity for PDZ3 is determined by the -1 position of the CRIPT C terminus as well as by amino acids upstream of the final four residues. These findings emphasize the exquisite specificity of PDZ recognition and indicate that the determinants of PDZ binding are more complicated than currently believed.

PSD-95, a core component of the PSD, is virtually insoluble in nondenaturing detergents (Cho et al., 1992, Allison et al., 1998), indicating a tight association with the cytoskeleton. Furthermore, the putative channel clustering and targeting function of PSD-95 implies a

direct or indirect interaction with the cytoskeleton. Despite the identification of a variety of ligands for PSD-95 family proteins, however, the mechanism(s) by which PSD-95 is attached to the postsynaptic cytoskeleton remains unclear. We show here that CRIPT can induce the recruitment of PSD-95 to microtubules and that CRIPT is tightly associated with PSD-95 and tubulin in vivo. Thus CRIPT is a candidate molecule involved in the cytoskeletal anchoring of PSD-95.

## Results

### Isolation of CRIPT, a Highly Conserved Protein that Binds to PDZ3 of PSD-95

To identify proteins that bind to the third PDZ domain of PSD-95, we screened a rat brain cDNA library by the yeast two-hybrid system, using PDZ3 as bait (Figure 1A). From $2 \times 10^6$ clones, four copies of a single identical clone (clone 3.13) were isolated, which encoded the last 98 amino acids of a novel protein. The two-hybrid interaction is specific—clone 3.13 bound to PDZ3 from PSD-95 but not to a series of negative control baits. The 3.13 coding region terminates in the sequence glutamine-threonine-serine-valine (-QTSV), which is consistent with the PDZ-binding tetrapeptide consensus (-X(T/S)XV).

Clone 3.13 was used to isolate the full-length coding sequence of the gene by conventional hybridization screening. The entire open reading frame encodes a 101 amino acid protein with a predicted molecular weight of 11 kDa and no recognizable motifs or domains (Figure 1B). We termed this protein CRIPT (for cysteine-rich interactor of PDZ three). A BLAST search of the GenBank database did not reveal homology to any known proteins. However, proteins homologous to CRIPT were found encoded in human and *Arabidopsis thaliana* ESTs (expressed sequence tags) as well as in a *C. elegans* genomic clone (Figure 1B). CRIPT is remarkable for its high degree of conservation across species and phyla, with 68% identity (78% similarity) between the human and *Arabidopsis* sequences (Figures 1B and 1C). The greatest conservation is found in the N- and C-terminal regions of the protein, which contain several -CXXC- repeats. Northern blotting showed CRIPT mRNA to be expressed in all tissues examined, including brain (Figure 1D). The presence of two major CRIPT transcripts ($\sim$1 and $\sim$2 kb in size) is consistent with our finding of two different 3′ untranslated regions in cloned CRIPT cDNAs (data not shown).

### CRIPT Binds Specifically to PDZ3 of PSD-95 Family Proteins

Although CRIPT was isolated by its binding to PDZ3, its C-terminal sequence (-QTSV) seemed potentially capable of interacting with the other PDZ domains of PSD-95 (consensus binding sequence -X(T/S)XV). Therefore, we assayed CRIPT interaction with individual PDZ domains (PDZ1, PDZ2, and PDZ3) in the yeast two-hybrid system. A comparison of PDZ domain preference between CRIPT, NR2B, and Kv1.4 is shown in Figure 2A. Both Kv1.4 and NR2B bound strongly to PDZ1 and PDZ2 but showed no detectable interaction with PDZ3. On the other hand, CRIPT showed strongest binding to PDZ3 and weak or no binding to PDZ2 and PDZ1. Thus, in contrast to Shaker and NR2 subunits, CRIPT shows binding preference for PDZ3 over PDZ1/2. CRIPT also bound specifically and with similar efficiency to the PDZ3 domains of all other members of the PSD-95 family: chapsyn-110, SAP102, and SAP97 (data not shown; see below). Substituting the C-terminal valine of CRIPT with alanine ($CRIPT_{V101A}$) abolished its interactions with PDZ3 and PDZ2 domains (Figure 2A), confirming that the C-terminal sequence of CRIPT is critical for PDZ binding.

We independently confirmed selective and direct interaction between CRIPT and PDZ3 using filter overlay assays with purified bacterial fusion proteins (Figure 2B).

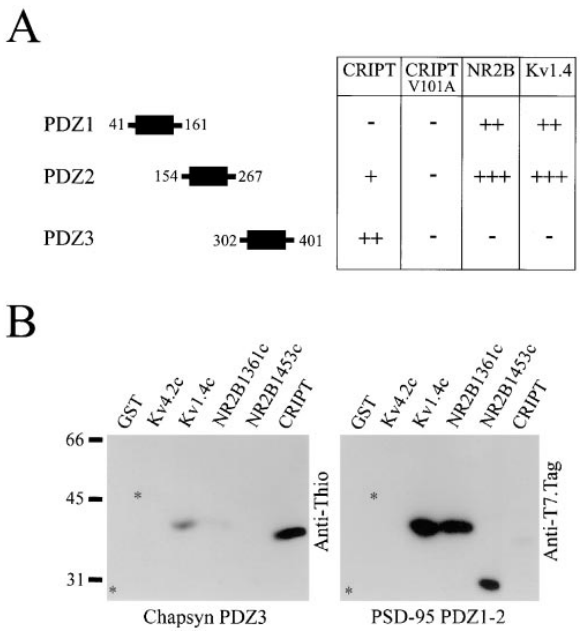


Figure 2. CRIPT Binds Specifically to the Third PDZ Domain of PSD-95 Family Proteins

(A) Interactions of individual PDZ domains of PSD-95 with CRIPT, a C-terminal mutant of CRIPT ($CRIPT_{V101A}$), NR2B, and Shaker channel Kv1.4 C termini. The yeast two-hybrid interaction was semiquantitated based on the degree of activation of the reporter gene β-galactosidase (time taken for colonies to turn blue in X-gal filter lift assays [Kim et al., 1995]: +++, <40 min; ++, 40–100 min; +, >100 min; -, no significant β-gal activity). Small numbers refer to amino acid residues.

(B) Filter overlay assay showing specific in vitro binding of PDZ3 to CRIPT. GST-fusion proteins of the C-terminal regions of Kv4.2, Kv1.4, NR2B, and CRIPT were separated by SDS-PAGE and transferred to nitrocellulose membranes. Left panel, filter was probed with soluble PDZ3 (a thioredoxin-fusion protein of PDZ3 from chapsyn-110), showing strong binding to CRIPT and weak binding to Kv1.4 and NR2B but no binding to Kv4.2 or GST alone. Right panel, identical filter probed with PDZ1–2 (a $H_6$-tagged fusion protein of the first two PDZ domains of PSD-95), demonstrating strong binding to Kv1.4 and NR2B but not to CRIPT, Kv4.2, or GST alone. NR2B1453c encodes a shorter version of the NR2B C terminus than NR2B1361c (Niethammer et al., 1996). Asterisks indicate positions of control Kv4.2 and GST-fusion proteins. The positions and comparable loading of all GST-fusion proteins was checked by stripping the filters and reprobing them with anti-GST antibodies (data not shown).

A

| Row | | Residue -9 | -8 | -7 | -6 | -5 | -4 | -3 | -2 | -1 | 0 | PDZ1 | PDZ2 | PDZ3 | PDZ3(N326S) |
|---|---|---|---|---|---|---|---|---|---|---|---|---|---|---|---|
| 1 | CRIPT | D | T | K | N | Y | K | Q | T | S | V | - | + | ++ | + |
| 2 | | D | T | K | N | Y | K | Q | T | D | V | + | ++ | - | ++ |
| 3 | | D | T | K | N | Y | K | E | T | D | V | +++ | +++ | - | +++ |
| 4 | | S | T | K | N | Y | K | Q | T | S | V | - | + | ++ | ++ |
| 5 | | S | N | K | N | Y | K | Q | T | S | V | - | + | ++ | + |
| 6 | | S | N | A | N | Y | K | Q | T | S | V | - | - | + | + |
| 7 | | S | N | A | K | Y | K | Q | T | S | V | - | - | + | + |
| 8 | | S | N | A | K | A | K | Q | T | S | V | - | - | - | - |
| 9 | | S | N | A | K | A | V | Q | T | S | V | - | + | - | - |
| 10 | | S | N | A | K | A | V | E | T | S | V | ++ | +++ | - | - |
| 11 | Kv1.4 | S | N | A | K | A | V | E | T | D | V | ++ | +++ | - | - |
| 12 | | S | N | A | K | A | V | E | T | D | A | - | - | - | n.d. |
| 13 | | S | N | A | K | A | V | E | A | D | V | - | - | - | n.d. |

B

| | | | | | | | | | | | $K_d$ (μM) |
|---|---|---|---|---|---|---|---|---|---|---|---|
| CRIPT | - | - | - | - | - | - | Q | T | S | V | 300 |
| | - | - | - | - | Y | K | Q | T | S | V | 2 |
| | - | T | K | N | Y | K | Q | T | S | V | 1 |
| NL | - | - | - | - | H | S | T | T | R | V | 120 |

Figure 3. The Determinants of CRIPT's Binding Preference for PDZ3

(A) Systematic mutation of CRIPT and Kv1.4 C-terminal sequences and their effects on binding to individual PDZ domains of PSD-95 and to $PDZ3_{N326S}$. The CRIPT C terminus was changed one residue at a time toward the sequence of Kv1.4 (row 1 down to row 3). The Kv1.4 C terminus was changed one residue at a time toward the sequence of CRIPT (row 11 up to row 4). The wild-type sequences are shown with a gray background. The presence of valine (V) at the 0 position and threonine (T) at the -2 position is shared between CRIPT and Kv1.4. V(0) to A mutants of both CRIPT and Kv1.4 do not bind to any PDZ domain (row 12; Figure 2A). Similarly, a T(-2) to A mutant of Kv1.4 cannot interact with the PSD-95 PDZ domains (row 13). Yeast two-hybrid interactions were measured as in Figure 2A. n.d., not done.

(B) Dissociation constants ($K_d$) for CRIPT and neuroligin (NL) C-terminal peptides binding to PDZ3 as measured by competitive fluorescence polarization assay.

A thioredoxin (Trx)-fusion protein containing PDZ3 of chapsyn-110/PSD-93 bound strongly to a GST-fusion of CRIPT and very weakly to the C termini of the Shaker subunit Kv1.4 and NR2B (Figure 2B, left). Conversely, a fusion protein containing the PDZ1 and PDZ2 domains of PSD-95 bound strongly to the C termini of Kv1.4 and NR2B, but not to CRIPT (Figure 2B, right). No binding was detectable with either fusion protein to GST alone or to the Shal-type $K^+$ channel subunit Kv4.2. Thus, both in vitro binding and yeast two-hybrid analysis indicate that CRIPT interacts preferentially with the PDZ3 domain of PSD-95 family proteins.

As another way to confirm and to extend the specificity of the CRIPT interaction, we performed a "reverse" yeast two-hybrid screen of the brain cDNA library, this time using CRIPT as bait. Twenty positives were isolated from $\sim 1.5 \times 10^6$ clones, 16 of which encoded for various members of the PSD-95 family of proteins (data not shown). In addition, the CRIPT two-hybrid screen also yielded four cDNA fragments encoding three novel proteins, each of which contains a PDZ domain. Interestingly, the PDZ domains of the three novel proteins show greater sequence similarity to PDZ3 of PSD-95 than to PDZ1 or PDZ2 (data not shown). Beyond supporting the PDZ3-binding specificity of CRIPT, these two-hybrid screen results also suggest the possibility of other binding partners for CRIPT among non-MAGUK proteins that contain PDZ3-like PDZ domains.

### Defining the Determinants of CRIPT's Binding Preference for PDZ3

The CRIPT C terminus (last four amino acids: -QTSV) binds selectively to the PDZ3 domain, whereas the similar C terminus of Kv1.4 (-ETDV) is specific for PDZ1 or PDZ2. What are the determinants of this differential PDZ binding? To address this question, we systematically mutated both CRIPT and Kv1.4 so that the sequence of their C-terminal tails was transformed stepwise from one protein into the other (Figure 3A). Significantly, starting from the CRIPT backbone (Figure 3, row 1), changing the -1 residue of CRIPT (serine) to that of Kv1.4 (aspartate) (QTSV→QTDV) abolished binding to PDZ3 while strengthening interaction with PDZ1 and PDZ2 (Figure 3A, row 2). Thus, the -1 position is critical for determining PDZ specificity, since a simple substitution at this position in CRIPT (QTSV→QTDV) changes the PDZ preference of CRIPT to that of Kv1.4. A further substitution of the -3 glutamine of CRIPT to glutamate (QTSV→ETDV) caused a further enhancement in PDZ1 and PDZ2 binding without rescuing PDZ3 interaction (Figure 3A, row 3). Thus, replicating the last four amino acids of Kv1.4 in the CRIPT backbone essentially converts CRIPT into Kv1.4 with respect to both PDZ-binding specificity and efficacy. The simple interpretation of these results is that the C-terminal tetrapeptide sequence is sufficient for determining PDZ binding, with the -1 and -3 positions specifying differential recognition between PDZ3 and PDZ1 or PDZ2. Note that the 0 (valine) and -2 (threonine) residues, which are conserved in both CRIPT and Kv1.4, are critical for binding to either PDZ2 or PDZ3 (Figures 2A and 3A; see Kim et al., 1995).

The situation becomes more complicated, however, when examining the effects of substitutions starting from the Kv1.4 backbone (Figure 3A, row 11, up). The converse substitution of the -1 position of Kv1.4 to that of CRIPT (ETDV→ETSV) did not promote PDZ3 binding (Figure 3A, row 10). PDZ3 binding was undetectable even after replicating the last four (-QTSV) or last five amino acids of CRIPT (-KQTSV) in the context of the Kv1.4 tail (Figure 3A, rows 9 and 8). In fact these mutations merely served to impair or abolish binding by PDZ1 and PDZ2. Since the C-terminal four or five amino acids of CRIPT were not sufficient to confer PDZ3 interaction, we continued to substitute residues further upstream in the Kv1.4 C-terminal tail. Only by changing the last six to seven residues of Kv1.4 to those of CRIPT were we able to detect PDZ3 binding in the two-hybrid system (Figure 3A, rows 6 and 7). Converting the PDZ binding behavior of the Kv1.4 C-terminal tail into that of the CRIPT C-terminal tail required changing the last eight

to nine residues (Figure 3A, rows 4 and 5). In contrast to PDZ2 binding, then, these results indicate that PDZ3 specificity is dependent on residues upstream of the C-terminal tetrapeptide as well as on the -1 and -3 positions close to the C terminus.

The differential binding specificity of PDZ3 may be due in part to asparagine (N)-326 within the PDZ3 domain (position βB2 in the crystal structure of Doyle et al., 1996). In PDZ1 and PDZ2, the equivalent amino acid is serine. Indeed, substituting residue N326 of PDZ3 with serine made the mutant domain ($PDZ3_{N326S}$) behave in part like PDZ2. For instance, $PDZ3_{N326S}$ bound to the -QTDV and -ETDV tetrapeptides in the context of the CRIPT C-terminal tail just like PDZ2 (Figure 3A, rows 2 and 3). Interestingly, however, $PDZ3_{N326S}$ was unable to bind -ETDV in the context of native Kv1.4 (Figure 3A, row 11)! In fact, $PDZ3_{N326S}$ showed overriding specificity for CRIPT sequences upstream of the last four amino acids, behaving identically to PDZ3 with respect to mutations in the Kv1.4 background (Figure 3A, rows 4–11, compare PDZ3 and $PDZ3_{N326S}$). $PDZ3_{N326S}$ thus exhibits specificity features of both PDZ2 and PDZ3, but the PDZ3-like properties (compatibility with upstream sequences) override those of PDZ2 (preference for D at -1).

To quantitate rigorously the strength of the interaction between CRIPT and PDZ3 and the role of residues upstream of the terminal tetrapeptide, we used fluorescence polarization (an in-solution method) to measure binding affinities (Figure 3B). The isolated C-terminal tetrapeptide of CRIPT bound only weakly to PDZ3 from PSD-95 (-QTSV, dissociation constant [$K_d$] ~300 μM). Binding was enhanced when upstream amino acids were included in the CRIPT peptide; the hexamer -YKQTSV and the nonamer -TKNYKQTSV bound with $K_d$s of ~2 μM and ~1 μM, respectively. These physicochemical measurements support the conclusion from mutagenesis experiments (Figure 3A) that CRIPT interactions with PDZ3 involve more than just the last four amino acids. Compared with CRIPT, the C-terminal hexapeptide from another reported PDZ3-binding protein, neuroligin (Irie et al., 1997), showed a weaker binding affinity for PDZ3 ($K_d$ ~120 μM).

### Immunohistochemical Localization of CRIPT Protein in Rat Brain

If CRIPT interacts with PSD-95 in vivo, one would expect colocalization of these proteins in brain synapses. We used affinity purified antibodies 97/3 (raised against a CRIPT peptide) and 13/8 (raised against a Trx-fusion of CRIPT) for immunohistochemical localization of CRIPT in rat brain. These two independent antibodies gave essentially the same staining patterns (compare Figures 4C and 4D), strongly suggesting that they are recognizing authentic CRIPT in brain sections. Here we show mostly results with 97/3 because that antibody had a higher signal-to-noise ratio. CRIPT is widespread but differentially expressed at the regional level in rat brain (Figure 4A). CRIPT staining was particularly heavy in the hippocampus, moderate in the striatum and cortex, and modest in the midbrain. At the cellular level, CRIPT immunoreactivity is associated with neurons and is distributed in a somatodendritic pattern (see for example the pyramidal neurons of hippocampus [Figures 4F–4H] and cortex [Figures 4B–4E] and the Purkinje neurons of cerebellum [Figure 4I]). In addition to this somatodendritic pattern, CRIPT staining was also present in the neuropil (Figure 4E). At this level of resolution, the pattern of CRIPT staining is similar to that of PSD-95 in brain (Cho et al., 1992; Kim et al., 1996). This staining pattern is specifically abolished by preincubation of CRIPT antibodies with the immunogen peptide (Figure 4K).

### Subcellular Colocalization of CRIPT and PSD-95 by LM and Immunogold EM

To obtain higher subcellular resolution and to facilitate double labeling studies, we stained for CRIPT in hippocampal neuronal cultures (Figure 5). CRIPT showed a punctate pattern of dendritic immunoreactivity, which colocalized almost exactly with PSD-95, especially on dendritic spines (Figures 5A–5C). Moreover, the CRIPT puncta are at synapses, as indicated by the close apposition of CRIPT labeling to that of the presynaptic terminal marker SV2 (Figure 5I). In addition, there was diffuse CRIPT staining in cell bodies and dendrites (Figure 5D). Preincubation of the antibody with immunogen peptide abolished the punctate dendritic spine staining, indicating that the synaptic labeling is specific (Figures 5E–5H). The diffuse cytoplasmic staining was only partially competed by peptide. CRIPT resembles PSD-95 in being absent from inhibitory GABAergic synapses (the latter labeled with GAD antibodies; Figure 5J).

Immunogold electron microscopy (EM) affords the highest level of spatial resolution and was used to localize CRIPT in rat brain. Consistent results were obtained from hippocampal area CA1 (Figure 6A), layers II/III of neocortex (Figures 6B and 6C), and cerebellum and striatum (data not shown). In all regions, gold particles for CRIPT were associated most prominently with asymmetric synapses. Synaptic labeling for CRIPT was concentrated in the deep part of the PSDs and was generally sparser over the synaptic cleft and the presynaptic terminal. Labeling at a lower density was also seen at nonsynaptic plasma membranes and within dendritic shafts, consistent with the light microscopy (LM) findings. Significantly, not all synapses were labeled with CRIPT antibodies. CRIPT was found postsynaptically in spines (and sometimes on dendritic shafts) associated with asymmetric synapses. Symmetric (presumably inhibitory) synapses, however, were uniformly negative for CRIPT. In a very few synapses, only the presynaptic part was labeled. In these cases, labeling was scattered over the terminal without an obvious association with the presynaptic membrane or presynaptic dense projections. When primary antibody was omitted, gold particles were completely absent or very rare. When normal serum was substituted for primary antibody, sparse gold particles appeared scattered at random, showing no significant affinity for synaptic regions (data not shown). Quantitative measurements revealed that the distribution of gold particles was uniform tangentially across the synapse, declining rapidly near the edge of the PSD (Figure 6F). Particle density along the axodendritic axis peaked about 35 nm inside the postsynaptic membrane, coinciding roughly with the inner edge of the PSD (Figure 6E).

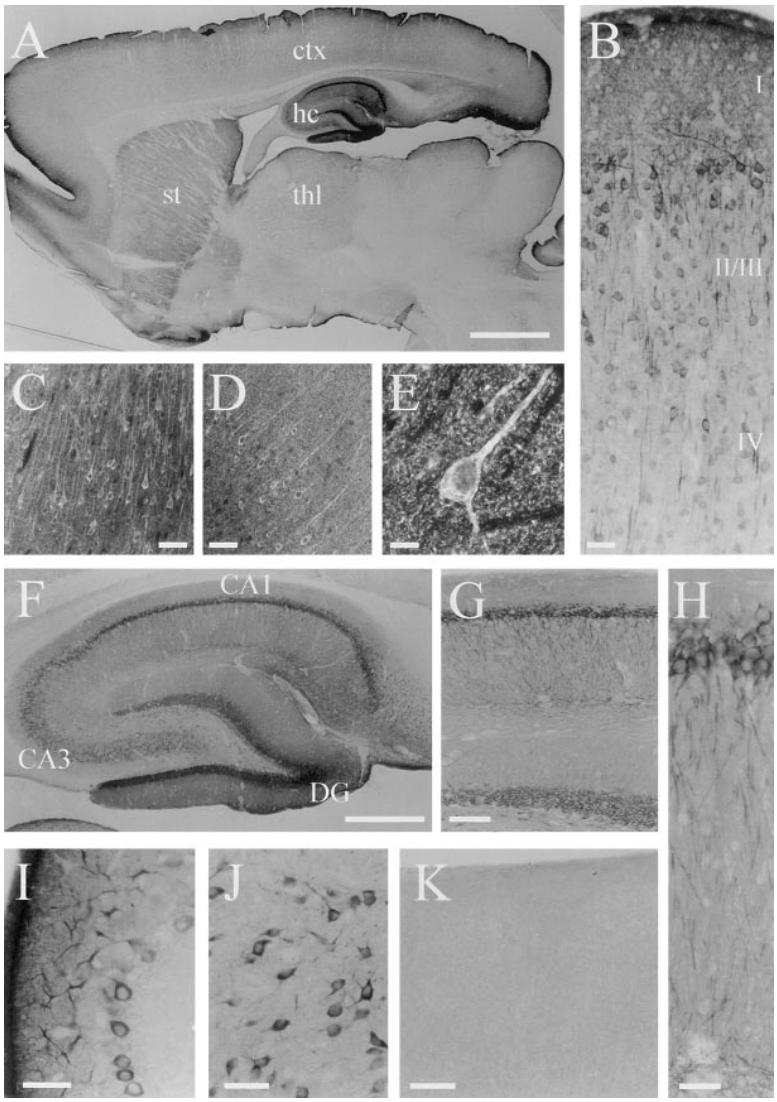


Figure 4. Immunohistochemical Localization of CRIPT in Rat Brain

Rat brain sections labeled with CRIPT antibodies and visualized by immunoperoxidase histochemistry (A, B, F–K) or immunofluorescence (C–E).

(A) Low magnification sagittal section. CRIPT staining is heavy in hippocampus (hc) and moderate in striatum (st), cortex (ctx), and thalamus (thl).

(B) Higher magnification view of neocortex showing CRIPT staining of pyramidal cells in a somatodendritic pattern. Cortical layers are indicated.

(C–E) Immunofluorescent images of cortical pyramidal cells in layer III showing somatodendritic staining of CRIPT. (C) and (E) were labeled with antibody 97/3, and (D) was labeled with antibody 13/8, demonstrating the similar staining pattern between the two independent antibodies.

(F–H) CRIPT staining is particularly prominent in hippocampus, where pyramidal neurons in areas CA3 through CA1 as well as granule cells in the dentate gyrus (DG) show strong somatodendritic labeling. (G) shows CA1 and one arm of the dentate gyrus; (H) shows a high-magnification view of pyramidal cell dendritic staining in CA1.

(I) Somatodendritic CRIPT immunoreactivity in Purkinje cells of the cerebellum.

(J) In the thalamus, scattered neurons are labeled.

(K) The staining pattern is abolished by preincubation of antibodies with CRIPT peptide (low-power view of cortex shown).

Scale bars = 2.5 mm, (A); 30 μm, (B) and (H); 50 μm, (C) and (D); 10 μm, (E); 800 μm, (F); 250 μm, (G); 100 μm, (I) and (J); 250 μm, (K).

In double labeling studies using different size gold particles, CRIPT was found to colocalize with PSD-95 in asymmetric synapses at the EM level (Figure 6D). Furthermore, CRIPT was postsynaptic to GABA-negative terminals only (presumably in excitatory synapses; data not shown). Taken together with the light microscopic findings, the immunoEM data indicate a colocalization of CRIPT with PSD-95 in excitatory synapses throughout the brain, consistent with a direct interaction of these proteins in the PSD.

### CRIPT Induces Redistribution of PSD-95 to Microtubules

To investigate a possible functional role for the interaction between CRIPT and PSD-95, we expressed these proteins heterologously in COS-7 cells. CRIPT, when expressed by itself, showed diffuse cytoplasmic staining with partial localization to an intracellular filamentous network (Figure 7B). This filamentous CRIPT staining is difficult to capture photographically, since it is somewhat obscured by the diffuse CRIPT staining. PSD-95, on the other hand, when expressed by itself is present diffusely throughout the cytoplasm with no detectable localization to a fibrillar network (Figure 7A; Kim et al., 1995). Upon coexpression with CRIPT, however, PSD-95 shifted its distribution from a diffuse to a filamentous network pattern (compare Figure 7C1 with 7A; see also Figures 8A and 8D). The PSD-95 relative chapsyn-110 showed a similarly striking subcellular redistribution from "diffuse" to "filamentous" when coexpressed with CRIPT (Figure 7D1). There was no apparent change in the distribution of CRIPT in PSD-95 or chapsyn-110 cotransfected cells; CRIPT remained largely diffuse with partial localization in a filamentous network that significantly overlapped with the filamentous staining pattern of redistributed PSD-95 (Figures 7C and 7D). Importantly, the redistribution of PSD-95 family proteins to a filamentous network is dependent on interaction with the CRIPT C terminus, because PSD-95 remained in a diffuse cytoplasmic pattern when coexpressed with $CRIPT_{V101A}$, a CRIPT mutant that cannot bind PSD-95 (Figure 7E1). Moreover, a mutant PSD-95 lacking PDZ3 (the CRIPT-binding domain) remains in a mostly diffuse distribution when cotransfected with CRIPT (Figure 8C).

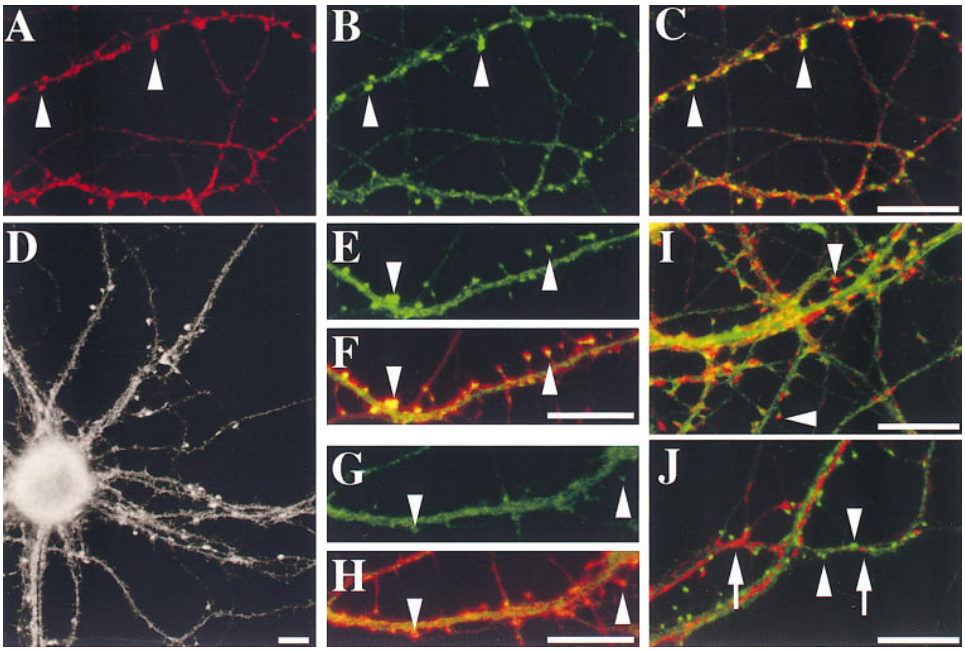


Figure 5. Concentration of CRIPT at Excitatory Synapses in Cultured Hippocampal Neurons

(A–C) Double staining with antibodies against PSD-95 (A) and CRIPT (B) shows that these proteins colocalize (C) especially on dendritic spines (arrowheads).

(D) Antibodies against CRIPT stain throughout the neuron, but immunoreactivity is concentrated in dendritic spines.

(E–H) Staining with antibodies against CRIPT (green in [E–H]) and rhodamine phalloidin to label concentrations of F-actin in spines (red in [F] and [H]) shows localization of CRIPT to dendritic spines (E and F). Spiny immunoreactivity of CRIPT is lost after preincubation of the antibody with the immunogenic peptide (G and H).

(I) Antibodies against the presynaptic marker SV2 (red) and CRIPT (green) show closely apposed signals, indicating that CRIPT punctate staining is synaptic (arrowheads).

(J) The lack of colocalization in the staining for GAD (red) and CRIPT (green) indicates that CRIPT (arrowheads) is not concentrated at inhibitory synapses (arrows).

Scale bars = 10 μm.

What is the molecular makeup of the filamentous network to which PSD-95 is recruited in the presence of CRIPT? Based on the hypothesis that the network was cytoskeletal in nature, we tried staining for actin, tubulin, and intermediate filaments (Figure 8). The PSD-95 fibrillar network induced by CRIPT showed no colocalization with the intermediate filament vimentin (Figure 8D) or with actin or endoplasmic reticulum markers (data not shown). Only the pattern of tubulin staining matched closely that of the PSD-95 filamentous network (Figure 8A), suggesting that PSD-95 was being recruited to microtubules in the presence of CRIPT.

CRIPT seems to reorganize the microtubule cytoskeleton independently of PSD-95 binding. In the absence of CRIPT, tubulin is present in thin fibers, often radiating out from the center of the cell (Figure 8A, upper cell). In the presence of CRIPT, the thickness and brightness of microtubule staining increases dramatically, and the microtubule network appears more convoluted (compare the tubulin staining of the untransfected upper cell with that of the lower transfected cell in Figure 8A; compare Figure 8E with 8F). This change in microtubule organization, and the redistribution of coexpressed PSD-95, is apparent in virtually all CRIPT-positive cells. The altered appearance of microtubules is found in cells transfected with CRIPT alone and is therefore not dependent on PSD-95 (Figures 8E and 8F). In keeping with this, the mutant $CRIPT_{V101A}$ (which cannot bind PSD-95) also causes a change in microtubule appearance that is indistinguishable from wild-type CRIPT (Figure 8B). However, PSD-95 does not redistribute to microtubules in $CRIPT_{V101A}$ expressing cells, presumably because $CRIPT_{V101A}$ cannot bind PSD-95 (Figure 8B). Similarly, when CRIPT is cotransfected with $PSD\text{-}95_{\Delta PDZ3}$ (a mutant which lacks PDZ3), the mutant PSD-95 remains for the most part diffusely distributed in the cytoplasm, even though the pattern of microtubule staining is altered (Figure 8C). Thus, the reorganization of the microtubule network and the recruitment of PSD-95 to these microtubules are separable functions that depend on different parts of the CRIPT protein.

### PSD-95 and Tubulin Can Be Coimmunoprecipitated with CRIPT from Rat Brain

CRIPT binds directly to PSD-95 in vitro; in addition, the data from heterologous cells suggest an interaction (which could be direct or indirect) between the CRIPT/PSD-95 complex and tubulin. To obtain in vivo evidence for these interactions, we performed coimmunoprecipitation experiments from rat brain extracts. In addition to CRIPT itself, CRIPT antibodies were able to coimmunoprecipitate PSD-95 and chapsyn-110 from solubilized synaptosomal membranes, indicating the existence of a biochemical complex containing CRIPT and PSD-95

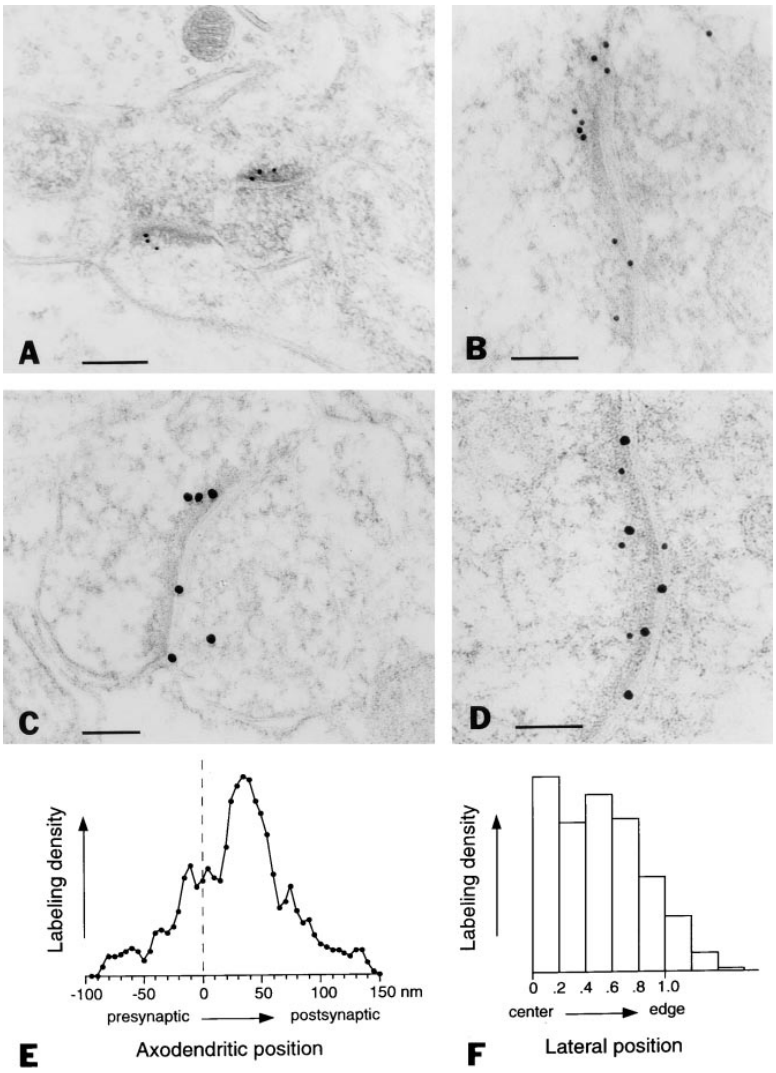


Figure 6. Immunogold EM Localization of CRIPT in Rat Brain

(A) Immunogold labeling for CRIPT in CA1 region of hippocampus (F(ab′)2, conjugated to 10 nm gold particles). The postsynaptic portions of two asymmetric synapses are immunopositive.

(B and C) Labeling of CRIPT in layer III of somatosensory cortex (12 nm gold in [B]; 18 nm gold in [C]). Labeling is concentrated over the postsynaptic density but may also be seen presynaptically.

(D) Double labeling for CRIPT (12 nm gold, small dots) and PSD-95 (18 nm gold, large dots) in layer III of somatosensory cortex showing colocalization in an asymmetric synapse.

(E) The distribution of immunogold particles along the axo-dendritic axis exhibited maximal density ~35 nm inside the postsynaptic membrane corresponding roughly to the inner edge of the postsynaptic density. Smaller peaks in density were seen at the presynaptic and postsynaptic membranes. Dashed line marks outer leaflet of postsynaptic membrane.

(F) Lateral distribution of particle density along the synapse. To permit comparison of locations in synapses with differing active zone lengths, lateral positions were normalized (see Experimental Procedures). Labeling was fairly uniformly distributed across the synapse, declining sharply at its edge.

Scale bars = 250 nm, (A); 100 nm, (B–D).

family proteins (Figure 9A). CRIPT could also be immunoprecipitated from cytosolic brain fractions; however, in this case it was not associated with PSD-95 or chapsyn-110, which are tightly membrane associated. In addition to PSD-95 family proteins, small amounts of NR2B and GKAP (a protein associated with the GK domain of PSD-95 [Kim et al., 1997; Naisbitt et al., 1997]) were present in CRIPT immunoprecipitates from membrane extracts (Figure 9A). These results are in keeping with CRIPT being indirectly associated with NMDA receptors and GKAP through their binding to PSD-95 family proteins. Consistent with this, NR2B antibodies were also able to coprecipitate PSD-95 and chapsyn-110 from membrane fractions (Figure 9A). However, neither CRIPT nor GKAP were detectable in NR2B precipitates, perhaps reflecting a lower efficiency of coimmunoprecipitation by NR2B antibodies. None of these synaptic proteins were immunoprecipitated by non-specific rabbit immunoglobulins (Figure 9A). GRIP and calmodulin, both abundant postsynaptic proteins, were not detectable in any of the immunoprecipitates (data not shown), indicating that the CRIPT antibodies were not simply immunoprecipitating large aggregates of the postsynapse but rather a specific subset of proteins. Preincubation of CRIPT antibodies with the immunogenic peptide abolished CRIPT immunoprecipitation as well as coimmunoprecipitation of PSD-95, chapsyn-110, and NR2B (Figure 9B).

Significantly, β-tubulin was also consistently coimmunoprecipitated from synaptosomal membrane extracts using CRIPT antibodies (Figure 9A). The precipitation of tubulin was due neither to nonspecific adhesiveness of tubulin nor to the presence of large aggregates of PSD proteins, since tubulin was only detected in CRIPT and not in nonimmune IgG or NR2B immunoprecipitates. Although CRIPT and NR2B can be indirectly linked through PSD-95, these coimmunoprecipitation data suggest a more direct association between tubulin and CRIPT than between tubulin and NR2 proteins. In summary, these findings support a biochemical association between CRIPT and PSD-95 family proteins and tubulin in synaptosomal membrane fractions.

## Discussion

### CRIPT, a Novel Protein of Neuronal Synapses

While a variety of ligands of the first two PDZ domains of the PSD-95 family of proteins have been described

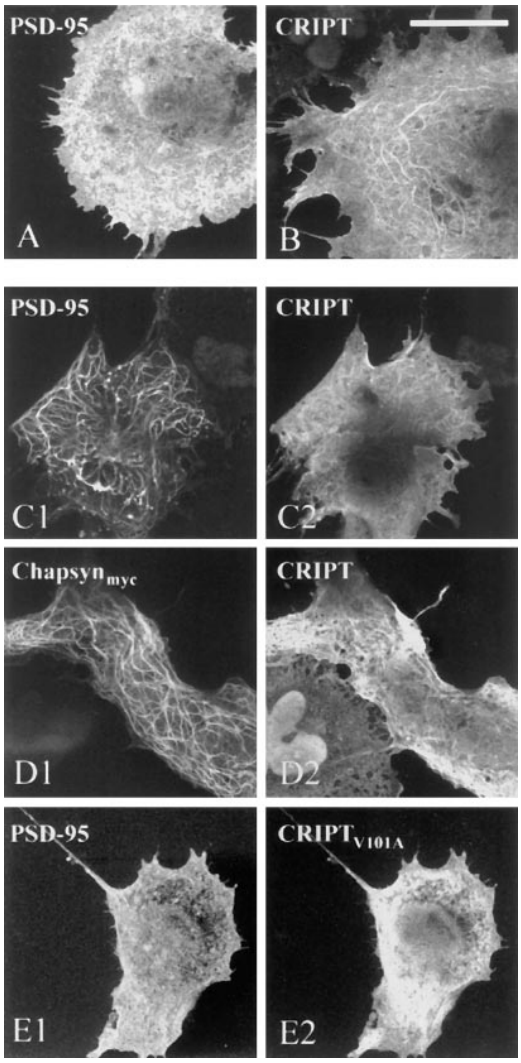


Figure 7. CRIPT Induces Subcellular Redistribution of PSD-95 to a Filamentous Network in Heterologous Cells

(A) When transfected in COS-7 cells by itself, PSD-95 is diffusely distributed in the cytoplasm.

(B) In cells transfected with CRIPT alone, CRIPT localizes partially to an intracellular fibrous network but is also diffusely distributed in the cytoplasm.

Panel pairs C1, C2; D1, D2; E1, E2 represent double-label images of single cells coexpressing the proteins indicated. The staining antibody is indicated in each panel.

(C) When coexpressed with CRIPT, PSD-95 shows a striking redistribution into a filamentous network (C1) where it overlaps with the partially filamentous CRIPT staining (C2).

(D) When coexpressed with CRIPT, Myc-tagged chapsyn-110 (labeled with Myc antibodies) also redistributes into a similar filamentous network (D1), where it overlaps with CRIPT (D2). When expressed by itself, chapsyn-110 is diffusely distributed like PSD-95 (not shown).

(E) When PSD-95 is coexpressed with CRIPT$_{V101A}$, PSD-95 remains diffusely distributed as if transfected by itself (E1), demonstrating the need for CRIPT binding for PSD-95 redistribution to occur.

Scale bar = 10 mm.

(Kim et al., 1995; Kornau et al., 1995; Matsumine et al., 1996; Niethammer et al., 1996; Kim et al., 1998), no proteins binding specifically to PDZ3 have been identified except for the transmembrane protein neuroligin (Irie et al., 1997). Here we report the characterization of CRIPT, a novel intracellular PDZ3 ligand that is concentrated in the PSD of excitatory synapses. The binding of the CRIPT C terminus to PDZ3 has been visualized at higher resolution (2 Å) than any other PDZ-mediated interaction, since it was the last nine amino acids of CRIPT that were used in the cocrystal of PDZ3 with its cognate peptide (Doyle et al., 1996).

Aside from what is known about its C terminus, little can be gleaned about the biochemical function of CRIPT from its sequence. The four -CXXC- motifs in CRIPT are reminiscent of the -CX$_{2,4}$C- motifs found in zinc fingers of transcription factors, but CRIPT lacks other critical zinc finger elements such as the histidine residues required for coordinating the metal ion (Berg, 1990). CXXC motifs are also found in the copper-binding pockets of CPx-type ATPases, in which only five residues (TCxSC) appear to be directly involved in making contact with the copper ion (Gitschier et al., 1998). In a variety of heavy metal–binding proteins, this binding motif is conserved in the sequence GMTCXXC. The CRIPT CXXC repeats seem to lack these conserved features for ion binding. Another possibility is that the CRIPT CXXC repeats are involved in intra- or intermolecular disulfide bonding. However, it will take future study to reveal the role of those motifs.

### PDZ Domain Specificity Depends on More than the Classical XT/SXV Motif

Many PDZ-containing proteins are localized at specialized submembranous sites, suggesting a central role for PDZ domains in assembling protein complexes involved in cell junction adhesion, transmembrane signaling, and protein anchoring (Sheng and Kim, 1996; Pawson and Scott, 1997; Ponting et al., 1997). The specialty of PDZ domains is to bind to specific sequences at the very C-terminal ends of interacting proteins. The consensus C-terminal sequence for binding to the PDZ domains of PSD-95 has been loosely summarized as -X(T/S)XV (or "tSXV"; Kornau et al., 1995). The differential PDZ binding of CRIPT (PDZ3 preferring) and Kv1.4 (PDZ2 preferring) allowed us to analyze systematically the basis of subtle sequence discrimination by PDZ domains. Our data indicate that the -1 position of the C-terminal peptide is a critical determinant of PDZ2 interaction. A negatively charged aspartate (D) in this -1 position is incompatible with PDZ3 while favoring PDZ2 binding. This mutagenesis result agrees with random peptide library screening with PDZ2, which enriched for aspartate and glutamate in the -1 position (Songyang et al., 1997). A glutamate (E) at -3 also seems to strengthen the interaction with PDZ2, but this may be an affinity effect rather than a specificity effect, since E at -3 is also compatible with PDZ3 binding (Songyang et al., 1997, Kim et al., 1998).

In contrast to PDZ2, specificity for PDZ3 is not primarily determined by the -1 residue of the X(T/S)XV motif, because a serine at this position does not overridingly specify PDZ3 binding. Rather, PDZ3 binding requires a compatible sequence upstream of -3 *in combination* with a suitable amino acid (such as serine) at -1. Whereas just the C-terminal four amino acids are sufficient for

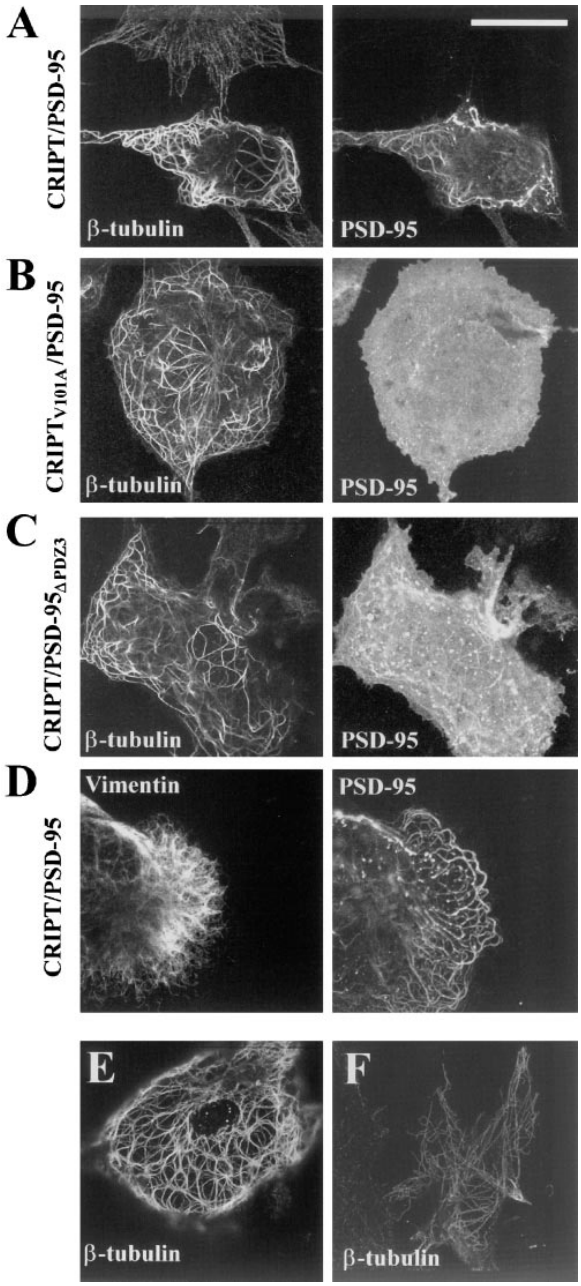


Figure 8. PSD-95 Colocalizes with Microtubules in CRIPT Transfected Cells

Panel pairs (A–D) represent single COS-7 cells transfected with PSD-95 or PSD-95$_{\Delta PDZ3}$ and CRIPT or CRIPT$_{V101A}$ as indicated next to each row and stained with antibodies against the proteins indicated within each panel.

(A) In COS-7 cells cotransfected with CRIPT and PSD-95, the redistributed PDS-95 (right) colocalizes with β-tubulin (left) in a thickened filamentous network. Note that two different cells are seen in the panel stained for tubulin. The upper cell is presumably an untransfected cell (no PSD-95 staining); it shows the typical fine appearance of the microtubule cytoskeleton in the absence of CRIPT.

(B) When PSD-95 is cotransfected with CRIPT$_{V101A}$, PSD-95 fails to redistribute and remains in a diffuse cytoplasmic pattern. Microtubules (β-tubulin staining), however, have a brighter, thickened appearance characteristic of that induced by CRIPT expression.

(C) In cells cotransfected with CRIPT and PSD-95$_{\Delta PDZ3}$, the mutant PSD-95 remains largely diffuse in the cytoplasm.

conferring PDZ2 binding, specific residues as far back as -7 appear to be involved in PDZ3 interaction. The importance of these upstream residues for PDZ3 binding is also indicated by the great increase in affinity shown by the C-terminal CRIPT hexapeptide and nonapeptide versus the tetrapeptide ligand. Both these results are consistent with the random peptide screening of Songyang et al. (1997), who found that PDZ3 selected for peptide ligands enriched in positively charged lysine (K) residues at the -4 through -8 positions. It is probably significant that lysine is indeed present at the -4 and -7 positions of CRIPT. The involvement of residues upstream of the C-terminal tetrapeptide in PDZ recognition has also received support from studies of the interaction between muscle sodium channels and the syntrophin PDZ domain (Gee et al., 1998; Schultz et al., 1998). The syntrophin PDZ domain is relatively similar to PDZ3 of PSD-95 in primary structure, and it also prefers lysine (K) or arginine (R) in the -4 position. Interestingly, the PDZ3 domains of Dlg/PSD-95 family proteins and the PDZ domain of syntrophins contain a conserved glutamate at position BC2 (in the loop between the βB and βC strands) that is situated close to the side chain of the -4 residue (Doyle et al., 1996; Songyang et al., 1997). The first two PDZ domains of the PSD-95 family, on the other hand, carry a glycine or proline residue at the equivalent position (BC8 in Doyle et al., 1996). Glu-BC2 in PDZ3 and syntrophin PDZs thus represents a good candidate for mediating charge-based interactions with positive side chains at the -4 position, selecting for lysine/arginine rather than for the hydrophobic residues found at that position in Kv1.4 and NR2A/B.

What part of the PDZ domain recognizes the -1 residue of the C-terminal peptide? Two candidate PDZ3 domain residues that might "see" the -1 position are βC5 and βB2 (Doyle et al., 1996). Both residues are part of the binding pocket near the -1 side chain (Songyang et al., 1997) and are different between PDZ3 (phenylalanine and asparagine, respectively) and PDZ2 (lysine and serine). Indeed, when we substituted N326 with its PDZ2 equivalent, the altered PDZ3 could bind to -ETDV in the context of the CRIPT tail. However, this N326S mutant PDZ3 still showed overriding specificity for CRIPT sequences upstream of the last four amino acids, since it could not bind to -ETDV in the context of native Kv1.4. Thus, N326 is involved in the recognition of the -1 position but not of residues upstream of -3. Overall, these data reveal the fine specificity of recognition by PDZ domains and begin to uncover the molecular basis for how PDZs discriminate between related C-terminal sequences.

The affinity of PDZ3 binding to CRIPT reported here ($K_d \sim 10^{-6}$ M) is substantially lower than that previously

(D) Lack of overlap of the intermediate filament vimentin and PSD-95 in CRIPT/PSD-95 cotransfected cells demonstrates that PSD-95 does not associate with this intermediate filament.

(E and F) Further examples of the effect of CRIPT on microtubule staining pattern shown in a cell transfected with CRIPT (E) compared to an untransfected cell (F).

Scale bar = 10 μm.

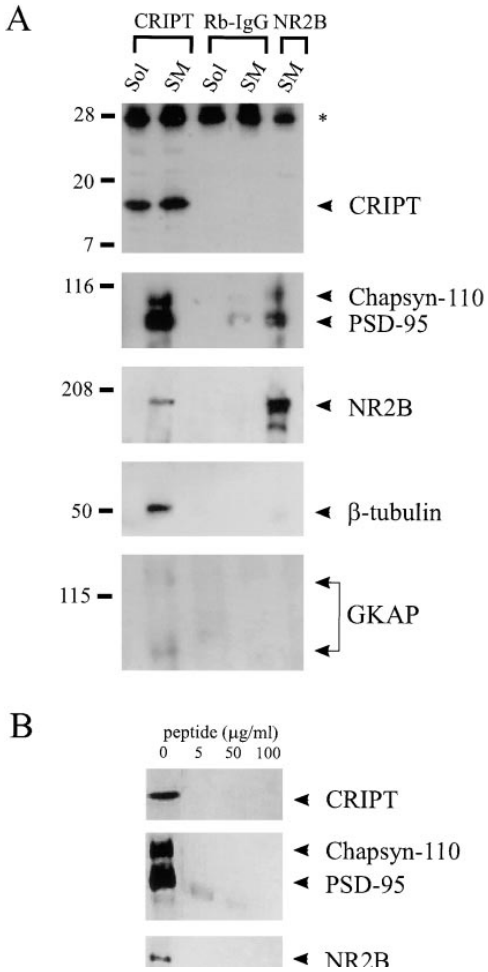


Figure 9. Coimmunoprecipitation of CRIPT, PSD-95, and Tubulin from Rat Brain

(A) Detergent extracts of rat whole brain synaptosomal membranes (SM) or soluble fractions (Sol) were immunoprecipitated with CRIPT antibodies, non-specific rabbit IgGs, or NR2B antibodies as indicated. The precipitates were immunoblotted for CRIPT, PSD-95/chapsyn-110, NR2B, β-tubulin, and GKAP. Neither GRIP or calmodulin, abundant postsynaptic proteins, were detectable in any of the immunoprecipitates (not shown). The asterisk indicates position of immunoglobulin light chains.

(B) Immunoprecipitation of CRIPT and coimmunoprecipitation of PSD-95, chapsyn-110, and NR2B from synaptosomal membrane extracts are blocked by preincubation of CRIPT antibodies with immunogenic peptide.

obtained for PDZ binding to NR2 or Shaker channel C termini using surface plasmon resonance or ELISA-style methods ($K_d$ in the order of $10^{-8}$ M or $10^{-7}$ M; Marfatia et al., 1996; Müller et al., 1996). This discrepancy could reflect real differences in the properties of PDZ2 versus PDZ3; however, both ELISA and surface plasmon resonance involve immobilization of one binding partner on a solid support. An in-solution measurement such as that afforded by fluorescence polarization may be more accurate. Micromolar binding constants are characteristic of SH3 domain interactions with their peptide ligands (Feng et al., 1995) and may be more appropriate than nanomolar affinities for dynamic protein–protein interactions in vivo.

### Functional Significance of the CRIPT/PSD-95 Interaction

Recent genetic studies (Tejedor et al., 1997; Thomas et al., 1997; Zito et al., 1997) have provided strong evidence that the Dlg/PSD-95 family of proteins plays an important role in the localization of their ion channel binding partners at synaptic sites. Presumably, this localization function depends on direct or indirect interactions of PSD-95 family proteins with the subsynaptic cytoskeleton. Several findings in this study suggest a possible role for CRIPT in the cytoskeletal attachment of PSD-95. First, in heterologous cells CRIPT causes a striking recruitment of PSD-95 to microtubules. Second, this redistribution requires CRIPT binding to PSD-95, since a binding-defective mutant $CRIPT_{V101A}$ was unable to induce this redistribution. One simple mechanism to explain this effect (the "bridging" model) is that CRIPT binds to microtubules independently of PSD-95, and PSD-95 is recruited to microtubules as a result of its binding to the CRIPT C terminus. Another possibility (the "activation" model) is that the binding of CRIPT to PDZ3 activates PSD-95 in such a way that PSD-95 now has affinity for microtubules. Future work is required to distinguish between these models. One piece of evidence in favor of the bridging model is that both CRIPT and $CRIPT_{V101A}$ appear to partially localize to microtubules in the absence of PSD-95 (Figure 7B; data not shown). Perhaps more significant is that CRIPT induces a reorganization of microtubules independently of its interaction with PSD-95, as evidenced, for instance, by the ability of $CRIPT_{V101A}$ to reorganize microtubules (Figure 8B). These data would be more consistent with a bridging model in which CRIPT interacts with PSD-95 via its C terminus and with microtubules via some other region, thereby recruiting PSD-95 to microtubules. Further supporting the bridging model is that known microtubule-binding proteins (such as cytoplasmic linker protein-115, which links dendritic lamellar bodies to microtubules) cause a macroscopic reorganization of tubulin in heterologous cells in a fashion remarkably similar to CRIPT (De Zeeuw et al., 1997). If a bridging model is correct for CRIPT action, it will be important to determine whether CRIPT interacts directly with microtubules (i.e., tubulin) or indirectly via specific microtubule-associated proteins.

Consistent with the involvement of CRIPT in cytoskeletal attachment of PSD-95 in vivo is the specific coimmunoprecipitation of tubulin with PSD-95 and CRIPT from synaptosomal membranes. This finding is compatible with either a bridging or an activation model for CRIPT action. Whichever is the case, given that CRIPT and PSD-95 are concentrated in the PSD, the general hypothesis would be that CRIPT mediates or regulates PSD-95 interaction with microtubules at postsynaptic sites. Certainly, microtubules are abundant in the dendritic shaft and could interact with CRIPT/PSD-95 localized in the PSDs of excitatory shaft synapses. In inhibitory glycinergic synapses, which are typically present on dendritic shafts, a microtubule-binding protein, gephyrin, links the glycine receptor to postsynaptic microtubules (Kirsch et al., 1991; Meyer et al., 1995).

An apparent problem with the above hypothesis is that microtubules are thought to be sparse or absent

from dendritic spines (Harris and Kater, 1994), where the majority of PSD-95 and CRIPT is found. Tubulin, on the other hand, is generally believed to be a major PSD protein in dendritic spines, although there has been debate as to the exact amount in the PSD and the role it may play there (Walters and Matus, 1975; Kelly and Cotman, 1978; Carlin et al., 1982; Cho et al., 1992; Harris and Kater, 1994). It is possible that tubulin exists in the PSD in an alternative morphological or polymerized state (Kelly and Cotman, 1978; Chang et al., 1997) while retaining a cytoskeletal function. In this regard, it is interesting that the microtubule-associated protein MAP2 has also been immunolocalized to spine PSDs despite the apparent absence of local microtubules. Therefore, a hypothesis worth pursuing is that CRIPT links PSD-95 to an atypical tubulin-based cytoskeleton at the PSD of dendritic spines.

The prevailing molecular view of PSD organization is that a local concentration of PDZ-containing proteins (like PSD-95) acts as an extended multimodular scaffold around which are docked specific sets of membrane proteins and associated intracellular signaling molecules (reviewed in Kennedy, 1997). However, little is known about the sequence of events in the assembly of the PSD or about the functional relationships of the various protein–protein interactions in the PSD. For instance, do the postsynaptic receptor/channels recruit PSD-95 to the postsynaptic membrane, or does a preformed PSD-95 lattice anchor the later-arriving receptor/ion channels? The latter is suggested by the finding that PSD-95 and GKAP are clustered at synaptic sites in cultured neurons before NMDA receptors (Rao et al., 1998), but it is possible that other uncharacterized ligands of PSD-95 gather at synapses prior to PSD-95. It will be important to determine the pattern of CRIPT accumulation during development of the synapse and to assess the effects of CRIPT on PSD-95-ion channel interactions; such studies will shed more light on the functional relationships between postsynaptic proteins.

CRIPT is widely expressed outside of the brain and is likely to interact with other specific proteins in those tissues where PSD-95 is not found. It is possible that CRIPT may regulate the microtubule association of a variety of PDZ-containing proteins in diverse tissues (potential candidates include the three novel PDZ-containing proteins isolated by the CRIPT two-hybrid screen). CRIPT may thus represent a new class of cytoskeletal linker proteins; its striking sequence conservation between animals and plants and its widespread tissue expression may reflect a fundamental role in cytoskeletal–membrane interactions.

## Experimental Procedures

### Yeast Two-Hybrid

Yeast two-hybrid screens were performed using the L40 yeast strain harboring the reporter genes *HIS3* and β-galactosidase (β-gal) under the control of upstream LexA-binding sites (Bartel et al., 1993; Hollenberg et al., 1995; Niethammer and Sheng, 1998). The PDZ3 bait consisted of amino acids 302–401 of PSD-95 fused to the lexA DNA-binding domain in vector pBHA. The CRIPT screen was similarly performed with CRIPT amino acids 4–101. A rat brain cDNA library constructed in GAL4-activation domain vector pGAD10 (Clontech Laboratories, Palo Alto, CA) was screened with both baits. Two-hybrid constructs of the individual PDZ domains of PSD-95 have been described (Niethammer et al., 1996). The $PDZ3_{N326S}$ mutant was generated using the Transformer site-directed mutagenesis kit (Clontech Laboratories, Palo Alto, CA). C-terminal mutants of CRIPT and Kv1.4 were generated by PCR using specific mutant primers and subcloned into vector pBHA.

### CRIPT Cloning and Northern Analysis

The original cDNA clone of CRIPT isolated from the yeast two-hybrid screen (clone 3.13) contained an open reading frame with stop codon and the entire 3′ untranslated region, but no obvious N-terminal. The open reading frame plus the first 200 nucleotides of the 3′ untranslated region of clone 3.13 was used to probe a rat hippocampus λZAPII cDNA library (Stratagene, La Jolla, CA). One of the isolated phage library clones contained an in-frame stop codon in its 5′ end, so we assigned the putative translation start site to the next methionine, which was in a good Kozak consensus.

For Northern analysis, rat poly(A) mRNA Multi Tissue Northern (Clontech Laboratories, Palo Alto, CA) was probed with $^{32}$P-labeled cDNA clone 3.13 and washed at 50°C in 0.1× SSC, 0.1 % SDS.

### Fusion Proteins and In Vitro Binding

Filter overlay assays were performed as previously described (Li et al., 1992; Niethammer et al., 1996). Full-length CRIPT and the C-terminal tails of NR2B (residues 1361–1482), NR2B (residues 1453–1482), Kv4.2 (residues 409–548), and Kv1.4 (residues 568–655) were subcloned into GST-fusion vector pGEX-4T-1 (Pharmacia, Uppsala, Sweden). GST-fusion proteins were prepared as crude bacterial lysates, separated by SDS-PAGE electrophoresis, transferred to nitrocellulose, and incubated with 0.5 μg/ml hexahistidine ($H_6$)-tagged fusion protein of the first two PDZ domains of PSD-95 (amino acids 41–267; Kim et al., 1995) or Trx-fusion protein of PDZ3 of chapsyn-110 (amino acids 421–500). Bound $H_6$-PSD-95 PDZ1–2 was detected by mouse monoclonal anti-T7. Tag antibodies (Novagen, Madison, WI) and bound Trx-chapsyn PDZ3 were detected by anti-thio antibody (Invitrogen, San Diego, CA). HRP-conjugated secondary antibodies and ECL chemiluminescence (Amersham, Arlington Heights, IL) were used to visualize the bands.

A competitive fluorescence polarization assay was performed as previously described for SH3 domains (Feng et al., 1995). Briefly, the assay used the fluorescently labeled peptide fluorescein carbonyl-YKQTSV-OH (Fl-YKQTSV). The affinity of Fl-YKQTSV for the PDZ domain was determined by measuring the fluorescence polarization at different concentrations of Fl-YKQTSV. The $K_d$ for Fl-YKQTSV and PDZ3 of PSD-95 was found to be 16 μM. Fluorescence-polarization values at different concentrations of the unlabeled peptides QTSV, YKQTSV, TKNYKQTSV (synthesized as in Feng et al., 1995), and HSTTRV (synthesized by QCB, Hopkinton, MA) were measured at fixed concentrations of PDZ3 (16 μM) and Fl-YKQTSV (1 μM). The dissociation constants were calculated based on competition as described (Feng et al., 1995). All measurements were repeated twice.

### Antibodies

Multiple rabbit CRIPT antisera were raised against a fusion protein and a peptide of CRIPT. The CRIPT fusion protein (amino acids 4–101 of CRIPT fused to thioredoxin) was constructed by subcloning this segment of the CRIPT cDNA into pET-32a(+) (Novagen, Madison, WI). The resulting fusion protein was purified by Ni-NTA affinity chromatography (ProBond Resin, Invitrogen, Carlsbad, CA). Two rabbits were immunized, and the antisera were affinity purified over CRIPT-Trx fusion proteins coupled to Sulfolink columns (Pierce, Rockford, IL), generating antibodies 12/8 and 13/8. Before purification the antisera were twice depleted of anti-thioredoxin antibodies on a thioredoxin protein column. Anti-peptide antibodies 96/3 and 97/3 were generated by immunizing two different rabbits with the synthetic peptide TSKKARFDPYGKNKFSTC, corresponding to CRIPT amino acids 41–58. These antibodies were also affinity purified over Sulfolink columns coupled to immunizing peptide.

### Immunoprecipitation

Crude synaptosomal membrane and cytosolic fractions were isolated from rat brain as described (Sheng et al., 1992; Kim et al., 1996). Immunoprecipitations were performed as described (Lau et al., 1996). Briefly, membrane or cytosolic fractions (500 μg total

protein) were solubilized in buffer containing 1% SDS, neutralized with 5 vol of 2% Triton X-100, and incubated with primary antibodies (5–10 mg) for 2 hr at 4°C. For the competition experiments, antibodies were preincubated with immunogenic peptide for 1 hr before being added. Immune complexes were precipitated with protein A Sepharose (Pharmacia), eluted with SDS sample buffer, and processed for Western blot analysis. The filters were probed with affinity purified rabbit antibodies against CRIPT, NR2B (Sheng et al., 1994), GKAP (Naisbitt et al., 1997), and GRIP (Mike Wyszynski and M. S., unpublished data) or mouse monoclonal antibodies against PSD-95 family proteins (Upstate Biotechnology, Lake Placid, NY), calmodulin (Upstate Biotechnology), and β-tubulin (Sigma, St Louis, MO). Bands were visualized by HRP-conjugated secondary antibodies and ECL chemiluminescence (Amersham).

**LM and EM Immunohistochemistry of Brain**

For LM immunohistochemistry, pentobarbital-anaesthetized male Sprague-Dawley rats (200–400 g) were intracardially perfused with paraformaldehyde. Vibratome brain sections (30 μm thick) were processed for immunocytochemistry using diaminobenzidine (DAB) or nickel-intensified DAB, using standard avidin/biotin/peroxidase histochemistry. Best results were obtained with primary antibody 97/3 after permeabilizing the sections with 50% ethanol; different dilutions of both this antibody and of 96/3 gave qualitatively similar results. In the competition experiments, antibodies were preincubated with immunogen peptide for 2.5 hr. For immunofluorescence, 50 μm sections were stained with primary antibodies (97/3 and 13/8, 0.5 μg/ml) and visualized with FITC-conjugated secondary antibodies (Jackson ImmunoResearch).

For immunogold EM, eight animals were perfusion fixed with a mixture of paraformaldehyde and 0.1%–2.5% glutaraldehyde; their brains were postfixed for 2–4 hr. Vibratome sections (50 μm thick) were processed for osmium free embedment (Phend et al., 1995) with a heat-cured epoxy resin (Epon-Spurr) or with UV-cured acrylic (Lowicryl KM20). Sections from cerebral cortex, hippocampus, striatum, and cerebellar cortex were collected on nickel mesh grids. Postembedding immunocytochemistry was performed according to Phend et al. (1995). Secondary immunogold labeling was with 18 nm gold particles conjugated to anti-rabbit IgG. For highest sensitivity, 1 nm silver-enhanced gold-particles were also used; for optimal localization we used 10 nm gold particles conjugated to the F(ab′)2 fragment of IgG. Grids were examined on a JEOL 200CX transmission electron microscope at 80 kV accelerating voltage. For quantitatation, micrographs at 40,000×–72,000× original magnification were digitized, and measurements of positions and locations of all gold particles were made interactively with NIH image software running on a Macintosh platform. For each grid studied, only the first ten synapses that had clearly visible synaptic structures (presynaptic membrane, synaptic cleft, postsynaptic membrane, and postsynaptic density) labeled with at least one gold particle within 100 nm on either side of the postsynaptic membrane were considered. To define "axodendritic" position, the distance was measured between the center of each gold particle and the outer leaflet of the postsynaptic membrane. The lateral edges of the active zone (AZ) were defined by the points of disappearance of the PSD and not by the points where presynaptic and postsynaptic membranes meet (usually several nanometers further along the same line). In perforated synapses, the entire length of the synapse including all fragments with PSD and all perforations was measured as a single AZ. To define "lateral" synaptic position of a gold particle, the distance from each end of the AZ to a line drawn perpendicular to the line of the synapse and running through the center of the gold particle was measured. To permit comparison among synapses, lateral positions (L) were normalized: if $l_1$ and $l_2$ are the distances from each end of the AZ to the perpendicular line through the particle, then $L = |l_1 - l_2|/(l_1 + l_2)$.

**COS-7 Cell and Neuronal Cultures**

The expression constructs for PSD-95, chapsyn-110, and Myc-tagged chapsyn-110 have been described (Kim and Sheng, 1996; Kim et al., 1996). cDNAs for CRIPT and $CRIPT_{V101A}$ were subcloned into mammalian expression vector GW1-CMV (British Biotechnology). COS-7 cells were grown on poly-lysine coated coverslips and transfected at 40%–60% confluence using the lipofectamine method (GIBCO BRL). Cells were fixed 2 days after transfection in 2% paraformaldehyde, permeabilized with 0.1% Triton X-100, and stained with primary antibodies and with Cy3- or FITC-labeled secondary antibodies (Jackson Immunoresearch). The primary antibodies used were rabbit CRIPT antibodies 96/3 and 97/3 (1 μg/ml), guinea pig anti-PSD-95 antibody (1 μg/ml; Kim et al., 1995), mouse anti-Myc antibody (Santa Cruz Biotechnology), mouse anti-β-tubulin antibody (Sigma), and rabbit anti-vimentin antibody (gift of P. Hollenbeck, Purdue University). Immunofluorescence was captured with a Bio-Rad MRC 1000 confocal microscope.

Rat hippocampal cultures were prepared using previously described methods (Banker and Cowan, 1977; Goslin and Banker, 1991). Neurons were fixed at 21 days in culture in warm 4% paraformaldehyde, 4% sucrose in phosphate buffered saline (PBS) for 15 min and permeabilized with 0.25% Triton X-100. Primary antibodies used were: CRIPT antibody 97/3, guinea pig anti-PSD-95 antiserum (1:300; Kim et al., 1995), a monoclonal antibody against SV2 (1;50; gift of K. M. Buckley, Harvard University), and a monoclonal antibody against glutamic acid decarboxylase (1:2; GAD-6, Developmental Studies Hybridoma Bank). Secondary antibodies were conjugated to FITC, Texas red, or AMCA (Vector Labs, Burlingame, CA). The coverslips were mounted in elvanol with 2% 1,4-diazabicyclo [2,2,2]octane. Fluorescent images were captured with a Zeiss Axioskop microscope (63×, 1.4 N. A. objective) and a Photometrics series 250 cooled CCD camera.

**Acknowledgments**

M. S. is an Assistant Investigator of the Howard Hughes Medical Institute. We thank Elaine Aidonidis for help with the manuscript and Jai Up Kim and Anna S. Serpinskaya for excellent technical support. T. M. K. acknowledges the Eli Lilly Predoctoral Fellowship administered by the Department of Chemistry and Chemical Biology at Harvard University. T. M. K is a graduate student in the laboratory of Stuart L. Schreiber and is grateful for his advice and support. This work received support from the Markey Charitable Trust (A. M. C.) and NIH grants NS33184 (A. M. C.), NS29879 (R. J. W.), and NS35050 (M. S.).

Received January 30, 1998; revised March 16, 1998.

**References**

Allison, D.W., Gelfand, V.I., Spector, I., and Craig, A.M. (1998). Role of actin in anchoring postsynaptic receptors in cultured hippocampal neurons: differential attachment of NMDA versus AMPA receptors. J. Neurosci., in press.

Anderson, J.M. (1996). Cell signaling: MAGUK magic. Curr. Biol. *6*, 382–384.

Banker, G.A., and Cowan, W.M. (1977). Rat hippocampal neurons in dispersed cell culture. Brain Res. *126*, 397–425.

Bartel, P.L., Chien, C.-T., Sternglanz, R., and Fields, S. (1993). Using the 2-Hybrid System to Detect Protein–Protein Interactions in Cellular Interactions in Development: A Practical Approach, D.A. Hartley, ed. (Oxford: Oxford University Press).

Berg, J.M. (1990). Zinc finger domains: hypotheses and current knowledge. Annu. Rev. Biophys. Biophys. Chem. *19*, 405–421.

Brenman, J.E., and Bredt, D.S. (1997). Synaptic signaling by nitric oxide. Curr. Opin. Neurobiol. *7*, 374–378.

Brenman, J.E., Chao, D.S., Gee, S.H., McGee, A.W., Craven, S.E., Santillano, D.R., Wu, Z., Huang, F., Xia, H., Peters, M.F., et al. (1996a). Interaction of nitric oxide synthase with the postsynaptic density protein PSD-95 and a1-syntrophin mediated by PDZ domains. Cell *84*, 757–767.

Brenman, J.E., Christopherson, K.S., Craven, S.E., McGee, A.W., and Bredt, D.S. (1996b). Cloning and characterization of postsynaptic density 93, a nitric oxide synthase interacting protein. J. Neurosci. *16*, 7407–7415.

Carlin, R.K., Grab, D.J., and Siekevitz, P. (1982). Postmortem accumulation of tubulin in postsynaptic density preparations. J. Neurochem. *38*, 94–100.

Chang, Y.-C., Chiang, S.-F., Lai, S.-L., and Sun, S.H. (1997). Novel cystein-rich proteins in the postsynaptic densities. Soc. Neurosci. *23*, 578.13.

Cho, K.-O., Hunt, C.A., and Kennedy, M.B. (1992). The rat brain postsynaptic density fraction contains a homolog of the *Drosophila* discs-large tumor suppressor protein. Neuron *9*, 929–942.

Cohen, N.A., Brenman, J.E., Snyder, S., and Bredt, D.S. (1996). Binding of the inward rectifier $K^+$ channel Kir 2.3 to PSD-95 is regulated by protein kinase A phosphorylation. Neuron *17*, 759–767.

De Zeeuw, C.I., Hoogenraad, C.C., Goedknegt, E., Hertzberg, E., Neubauer, A., Grosveld, F., and Galjart, N. (1997). CLIP-115, a novel brain-specific cytoplasmic linker protein, mediates the localization of dendritic lamellar bodies. Neuron *19*, 1187–1199.

Doyle, D.A., Lee, A., Lewis, J., Kim, E., Sheng, M., and MacKinnon, R. (1996). Crystal structures of a complexed and peptide-free membrane protein-binding domain: molecular basis of peptide recognition by PDZ. Cell *85*, 1067–1076.

Ehlers, M.D., Mammen, A.L., Lau, L.-F., and Huganir, R.L. (1996). Synaptic targeting of glutamate receptors. Curr. Opin. Cell Biol. *8*, 484–489.

Feng, S., Kasahara, C., Rickles, R.J., and Schreiber, S.L. (1995). Specific interactions outside the proline-rich core of two classes of Src homology 3 ligands. Proc. Natl. Acad. Sci. USA *92*, 12408–12415.

Gee, S.H., Madhavan, R., Levinson, S.R., Caldwell, J.H., Sealock, R., and Froehner, S.C. (1998). Interaction of muscle and brain sodium channels with multiple members of the syntrophin family of dystrophin-associated protein. J. Neurosci. *18*, 128–137.

Gitschier, J., Moffat, B., Reilly, D., Wood, W.I., and Fairbrother, W.J. (1998). Solution structure of the fourth metal-binding domain from the Menkes copper-transporting ATPase. Nat. Struct. Biol. *5*, 47–54.

Goslin, K., and Banker, G. (1991). Culturing Nerve Cells, K. Goslin and G. Banker, eds. (Cambridge, MA: MIT Press).

Harris, K.M., and Kater, S.B. (1994). Dendritic spines: cellular specializations imparting both stability and flexibility to synaptic function. Annu. Rev. Neurosci. *17*, 341–371.

Hollenberg, S.M., Sternglanz, R., Cheng, P.F., and Weintraub, H. (1995). Identification of a new family of tissue-specific basic helix-loop-helix proteins with a two-hybrid system. Mol. Cell. Biol. *15*, 3813–3822.

Holmes, T.C., Fadool, D.A., Ren, R., and Levitan, I.B. (1996). Association of Src tyrosine kinase with a human potassium channel mediated by SH3 domain. Science *274*, 2089–2091.

Horio, Y., Hibino, H., Inanobe, A., Yamada, M., Ishii, M., Tada, Y., Satoh, E., Hata, Y., Takai, Y., and Kurachi, Y. (1997). Clustering and enhanced activity of an inwardly rectifying potassium channel, Kir4.1, by an anchoring protein, PSD-95/SAP90. J. Biol. Chem. *272*, 12885–12888.

Hsueh, Y.-P., Kim, E., and Sheng, M. (1997). Disulfide-linked head-to-head multimerization in the mechanism of ion channel clustering by PSD-95. Neuron *18*, 803–814.

Irie, M., Hata, Y., Takeuchi, M., Ichtchenko, K., Toyoda, A., Hirao, K., Takai, Y., Rosahl, T.W., and Südhof, T.C. (1997). Binding of neuroligins to PSD-95. Science *277*, 1511–1515.

Kelly, P.T., and Cotman, C.W. (1978). Characterization of tubulin and actin and identification of a distinct postsynaptic density polypeptide. J. Cell Biol. *79*, 173–183.

Kennedy, M.B. (1997). The postsynaptic density at glutamatergic synapses. Trends Neurosci. *20*, 264–268.

Kim, E., and Sheng, M. (1996). Differential $K^+$ channel clustering activity of PSD-95 and SAP97, two related membrane-associated putative guanylate kinases. Neuropharmacology *35*, 993–1000.

Kim, E., Niethammer, M., Rothschild, A., Jan, Y.N., and Sheng, M. (1995). Clustering of shaker-type $K^+$ channels by interaction with a family of membrane-associated guanylate kinases. Nature *378*, 85–88.

Kim, E., Cho, K.-O., Rothschild, A., and Sheng, M. (1996). Heteromultimerization and NMDA receptor-clustering activity of chapsyn-110, a member of the PSD-95 family of proteins. Neuron *17*, 103–113.

Kim, E., Naisbitt, S., Hsueh, Y.-P., Rao, A., Rothschild, A., Craig, A.M., and Sheng, M. (1997). GKAP, a novel synaptic protein that interacts with the guanylate kinase-like domain of the PSD-95/SAP90 family of channel clustering molecules. J. Cell Biol. *136*, 669–678.

Kim E., DeMarco, S.J., Marfatia, S.M., Chishti, A.H, Sheng, M., and Strehler, E.E. (1998). Plasma membrane $Ca^{2+}$ ATPase isoform 4b binds to membrane-associated guanylate kinase (MAGUK) proteins via their PDZ (PSD-95/Dlg/ZO-1) domains. J. Biol. Chem. *16*, 1591–1595.

Kirsch, J., Langosch, D., Prior, P., Littauer, U.Z., Schmitt, B., and Betz, H. (1991). The 93-kDa glycine receptor-associated protein binds to tubulin. J. Biol. Chem. *266*, 22242–22245.

Kistner, U., Wenzel, B.M., Veh, R.W., Cases-Langhoff, C., Garner, A.M., Appeltauer, U., Voss, B., Gundelfinger, E.D., and Garner, C.C. (1993). SAP90, a rat presynaptic protein related to the product of the *Drosophila* tumor suppressor gene *dlg*-A. J. Biol. Chem. *268*, 4580–4583.

Kornau, H.-C., Schenker, L.T., Kennedy, M.B., and Seeburg, P.H. (1995). Domain interaction between NMDA receptor subunits and the postsynaptic density protein PSD-95. Science *269*, 1737–1740.

Kornau, H., Seeburg, P., and Kennedy, M. (1997). Interaction of ion channels and receptors with PDZ domain proteins. Curr. Opin. Neurobiol. *7*, 368–373.

Lau, L.-F., Mammen, A., Ehlers, M.E., Kindler, S., Chung, W.J., Garner, C.C., and Huganir, R.L. (1996). Interaction of the *N*-methyl-D-aspartate receptor complex with a novel synapse-associated protein, SAP102. J. Biol. Chem. *271*, 21622–21628.

Li, M., Jan, Y.N., and Jan, L.Y. (1992). Specification of subunit assembly by the hydrophilic amino-terminal domain of the shaker potassium channel. Science *257*, 1225–1230.

Lue, R.A., Marfatia, S.M., Branton, D., and Chishti, A.H. (1994). Cloning and characterization of hdlg: the human homologue of the *Drosophila* discs large tumor suppressor binds to protein 4.1. Proc. Natl. Acad. Sci. USA *91*, 9818–9822.

Marfatia, S.M., Cabral, J.H.M., Lin, L., Hough, C., Bryant, P.J., Stolz, L., and Chishti, A.H. (1996). Modular organization of the PDZ domains in the human discs-large protein suggests a mechanism for coupling PDZ domain-binding proteins to ATP and the membrane cytoskeleton. J. Cell Biol. *135*, 753–766.

Matsumine, A., Ogai, A., Senda, T., Okumura, N., Satoh, K., Baeg, G.-H., Kawahara, T., Kobayashi, S., Okada, M., Toyoshima, K., and Akiyama, T. (1996). Binding of APC to the human homolog of the *Drosophila* discs large tumor suppressor protein. Science *272*, 1020–1023.

Meyer, G., Kirsch, J., Betz, H., and Langosch, D. (1995). Identification of a gephyrin binding motif on the glycine receptor β subunit. Neuron *15*, 563–572.

Müller, B.M., Kistner, U., Veh, R.W., Cases-Langhoff, C., Becker, B., Gundelfinger, E.D., and Garner, C.C. (1995). Molecular characterization and spatial distribution of SAP97, a novel presynaptic protein homologous to SAP90 and the *Drosophila* discs-large tumor suppressor protein. J. Neurosci. *15*, 2354–2366.

Müller, B.M., Kistner, U., Kindler, S., Chung, W.J., Kuhlendahl, S., Lau, L.-F., Veh, R.W., Huganir, R.L., Gundelfinger, E.D., and Garner, C.C. (1996). SAP102, a novel postsynaptic protein that interacts with the cytoplasmic tail of the NMDA receptor subunit NR2B. Neuron *17*, 255–265.

Naisbitt, S., Kim, E., Weinberg, R.J., Rao, A., Yang, F.-C., Craig, A.M., and Sheng, M. (1997). Characterization of guanylate kinase-associated protein, a postsynaptic density protein at excitatory synapses that interacts directly with posysynaptic density-95/synapse-associated protein 90. J. Neurosci. *17*, 5687–5696.

Niethammer, M., and Sheng, M. (1998). Identification of ion channel–associated proteins using the yeast two-hybrid system. Methods Enzymol., in press.

Niethammer, M., Kim, E., and Sheng, M. (1996). Interaction between the C terminus of NMDA receptor subunits and multiple members of the PSD-95 family of membrane-associated guanylate kinases. J. Neurosci. *16*, 2157–2163.

Pawson, T., and Scott, J.D. (1997). Signaling through scaffold, anchoring, and adaptor proteins. Science *278*, 2075–2080.

Phend, K.D., Rustioni, A., and Weinberg, R.J. (1995). An osmium-free method of Epon embedment that preserves both ultrastructure and antigenicity for postembedding immunocytochemistry. J. Histochem. Cytochem. *43*, 283–292.

Ponting, C.P., Phillips, C., Davies, K.E., and Blake, D.J. (1997). PDZ domains: targeting signaling molecules to sub-membranous sites. BioEssays *19*, 469–479.

Rao, A., Kim, E., Sheng, M., and Craig, A.M. (1998) Heterogeneity in the molecular composition of excitatory postsynaptic sites during development of hippocampal neurons in culture. J. Neurosci. *18*, 1217–1229.

Schultz, J., Hoffmüller, U., Krause, G., Ashurst, J., Macias, M.J., Schmieder, P., Schneider-Mergener, J., and Oschkinat, H. (1998). Specific interactions between the syntrophin PDZ domain and voltage-gated sodium channels. Nat. Struct. Biol. *5*, 19–24.

Sheng, M., and Kim, E. (1996). Ion channel associated proteins. Curr. Opin. Neurobiol. *6*, 602–608.

Sheng, M., and Wyszynski, M. (1997). Ion channel targeting in neurons. BioEssays *19*, 847–853.

Sheng, M., Tsaur, M.-L., Jan, Y.N., and Jan, L.Y. (1992). Subcellular segregation of two A-type $K^+$ channel proteins in rat central neurons. Neuron *9*, 271–284.

Sheng, M., Cummings, J., Roldan, L.A., Jan, Y.N., and Jan, L.Y. (1994). Changing subunit composition of heteromeric NMDA receptors during development of rat cortex. Nature *368*, 144–147.

Songyang, Z., Fanning, A.S., Fu, C., Xu, J., Marfatia, S.M., Chishti, A.H., Crompton, A., Chan, A.C., Anderson, J.M., and Cantley, L.C. (1997). Recognition of unique carboxyl-terminal motifs by distinct PDZ domains. Science *275*, 73–77.

Tejedor, F.J., Bokhari, A., Rogero, O., Gorczyca, M., Zhang, J., Kim, E., Sheng, M., and Budnik, V. (1997). Essential role for *dlg* in synaptic clustering of shaker $K^+$ channels in vivo. J. Neurosci. *17*, 152–159.

Thomas, U., Kim, E., Kuhlendahl, S., Ho Koh, Y., Gundelfinger, E.D., Sheng, M., Garner, C.C., and Budnik, V. (1997). Synaptic clustering of the cell adhesion molecule fasciclin II by discs-large and its role in the regulation of presynaptic structure. Neuron *19*, 787–799.

Tsunoda, S., Sierralta, J., Sun, Y., Bodner, R., Suzuki, E., Becker, A., Socolich, M., and Zuker, C.S. (1997). A multivalent PDZ-domain protein assembles signaling complexes in a G-protein-coupled cascade. Nature *388*, 243–249.

Walters, B.B., and Matus, A.I. (1975). Tubulin in postsynaptic junctional lattice. Nature *257*, 496–498.

Woods, D.F., and Bryant, P.J. (1991). The discs-large tumor suppressor gene of *Drosophila* encodes a guanylate kinase homolog localized at septate junctions. Cell *66*, 451–464.

Yu, X.M., Askalan, R., Keil, G.J., and Salter, M.W. (1997). NMDA channel regulation by channel-associated protein tyrosine kinase Src. Science *275*, 674–678.

Ziff, E.B. (1997). Enlightening the postsynaptic density. Neuron *19*, 1163–1174.

Zito, K., Fetter, R.D., Goodman, C.S., and Isacoff, E.Y. (1997). Synaptic clustering of fasciclin II and shaker: essential targeting sequences and role of dlg. Neuron *19*, 1007–1016.

**GenBank Accession Number**

The CRIPT sequence has been deposited in GenBank (accession number AF047384).